J. Nano- Electron. Phys.
2 (2010) No4, P. 153-168

PACS numbers: 75.70 – i, 75.70.Cn, 75.75. + a, 68.37.Lp

MAGNETORESISTIVE PROPERTIES OF Fe FILMS AND Fe-BASED MULTILAYERS

O.V. Synashenko, D.M. Kondrahova, I.Yu. Protsenko

Sumy State University,
2, Rimsky-Korsakov Str., 40007 Sumy, Ukraine
E-mail: protsenko@aph.sumdu.edu.ua

The investigation results of the size dependence of magnetoresistive effect are presented for Fe films prepared by the resistive sputtering method on a substrate heated to 400 *K. Correlation of magnetoresistance with structure and phase state was determined for multilayer film systems based on Fe and Cu or Cr subject to the thickness ratio of magnetic and non-magnetic layers. The thermal annealing influence on the magnetoresistance, induction of demagnetizing and saturation values was studied. The values of magnetoresistance to magnetic induction sensitivity were calculated.*

Keywords: *MAGNETORESISTANCE, INDUCTION OF DEMAGNETIZING, INDUCTION OF SATURATION, SENSITIVITY, SOLID SOLUTION.*

(Received 27 December 2010, in final form 17 January 2011)

1. INTRODUCTION

Magnetoresistive effect in thin ferromagnetic films is conditioned by the electron scattering by domain magnetic moments and walls, and in this case the effect value does not exceed (10^{-3}-10^{-2})%. Discovery of the giant magnetoresistance (GMR) phenomenon in nanoscale film systems (multilayers, spin-valves) based on ferromagnetic (Fe, Cu) and para- (Cu, Au, Ag) or antiferromagnetic (Cr) allowed to observe the magnetoresistive effect with considerably larger value (of the order of 1-100%). In such systems, in contrast to ferromagnetic films, the spin-dependent electron scattering by additional scatter centers (for example, ferromagnetic granules and magnetic/non-magnetic material interfaces) dominates.

The aim of our research is the study of the size dependence of the magnetoresistive effect in thin Fe films and Fe-based multilayers, as well as the influence of the thermal treatment of the samples on the effect value. Electron-microscope investigations allowed to determine the phase composition of the obtained samples and establish its correlation with magnetoresistive properties.

2. EXPERIMENTAL TECHNIQUE

Thin Fe films and multilayers based on Fe and Cu or Cr were obtained by the thermal evaporation method in the vacuum (pressure of the residual atmosphere is 10^{-3}-10^{-4} Pa) on the substrates (S) of amorphous glass-ceramic (for magnetoresistive investigations) and carbon films of the thickness of 20 nm (for electron-microscope investigations).

When obtaining multilayer film systems, condensation was performed layer-by-layer from two evaporators separated by a screen. Substrate with contact tracks and mask was fastened on a round table attached to a special electric motor intended for the movement in the vacuum plant VUP-5M. The motor speed was 30-90 rev/min. To prevent decrepitation of the films based on Cr and Fe, the substrate was heated up to the temperature 370-400 K using the molybdenum coil. Layer-by-layer condensation on the substrate took place in the evaporation zone of one of the metals. Thickness of separate layers was determined by the evaporation rate of the components and total thickness defined by the interferometric method using glass witnesses. This allowed to obtain film systems with different atomic concentrations of the components, which was defined by formula

$$c_i = \frac{\rho_i d_i \;/\; \mu_i}{\rho_1 d_1 \;/\; \mu_1 + \rho_2 d_2 \;/\; \mu_2},$$

where ρ_i and μ_i are the component density and molar mass, respectively.

Study of the magnetoresistive properties was performed at room temperature using two-point scheme in external magnetic field from 0 to 300 mT. In this case measurements were carried out in three geometries: longitudinal, when the magnetic-field vector **B** is directed along the current flow; transverse, when **B** is perpendicular to the current flow (in both cases **B** is parallel to the sample plane), and normal, when **B** is perpendicular to the plane. The value of magnetoresistance (MR) was determined as $\Delta R/R_s = (R(B) - R_s)/R_s$, where $R(B)$ are the current values of resistance of the film system in magnetic field; R_s is the resistance at the saturation field.

Annealing of the samples was carried out in the temperature range from 300 K to 900 K. Electron-microscope and electron-diffraction investigations were performed using the transmission electron microscope PEM-125K.

3. EXPERIMENTAL RESULTS

3.1 Thin Fe films

In Fig. 1 we present an example of magnetoresistive dependences for thin Fe film of the thickness of 11 nm. Results of the MR measurements in the unannealed and annealed to T_{ann} = 700 and 900 K states are shown in Table 1. As seen, in ferromagnetic Fe films one can observe the anisotropy of the field dependences $R(B)$ that is characterized by the negative magnetoresistive effect in the longitudinal geometry and by the positive one in the transverse and normal geometries. Thermal annealing of the samples leaded to a slight growth of the amplitude $\Delta R/R_s$ (T_{ann} = 700 K), to its decrease in the case T_{ann} = 900 K in the transverse geometry, and to a smooth fall of $\Delta R/R_s$ in the whole temperature range in the longitudinal and normal geometries (Fig. 2).

As it was noted by the authors of [1, 2], the coercitivity determined by the measurements of the change in the electrical resistance in magnetic field does not coincide with H_c obtained from the dependence of the magnetization **M** on the magnetic field strength **H**, but carries qualitative information about the thin film behavior during remagnetization. In our case, we will call the field induction, which is necessary for complete demagnetizing of the sample, the induction of demagnetizing and designate it B_c by analogy with the coercitivity. Data about the value of the induction of demagnetizing and saturation for thin Fe films unannealed and annealed to different temperatures is presented in Table 2 and shown in Fig. 3 and Fig. 4. Because of the absence of the coercitivity and magnetic saturation (in the studied range of the magnetic field) in the normal geometry, data is represented for two geometries, when **B** is parallel to the sample plane. In the considered thickness range, the value of induction of demagnetizing belongs to the interval (2,0-3,3) mT in the longitudinal geometry and (2,0-5,4) mT in the transverse one. Such difference in the values depending on the measurement geometry is also observed for the induction of saturation B_s. Preferential dominance of the values B_c and B_s in the transverse geometry can indicate the existence of the easy magnetization axis in thin Fe films along the current flow.

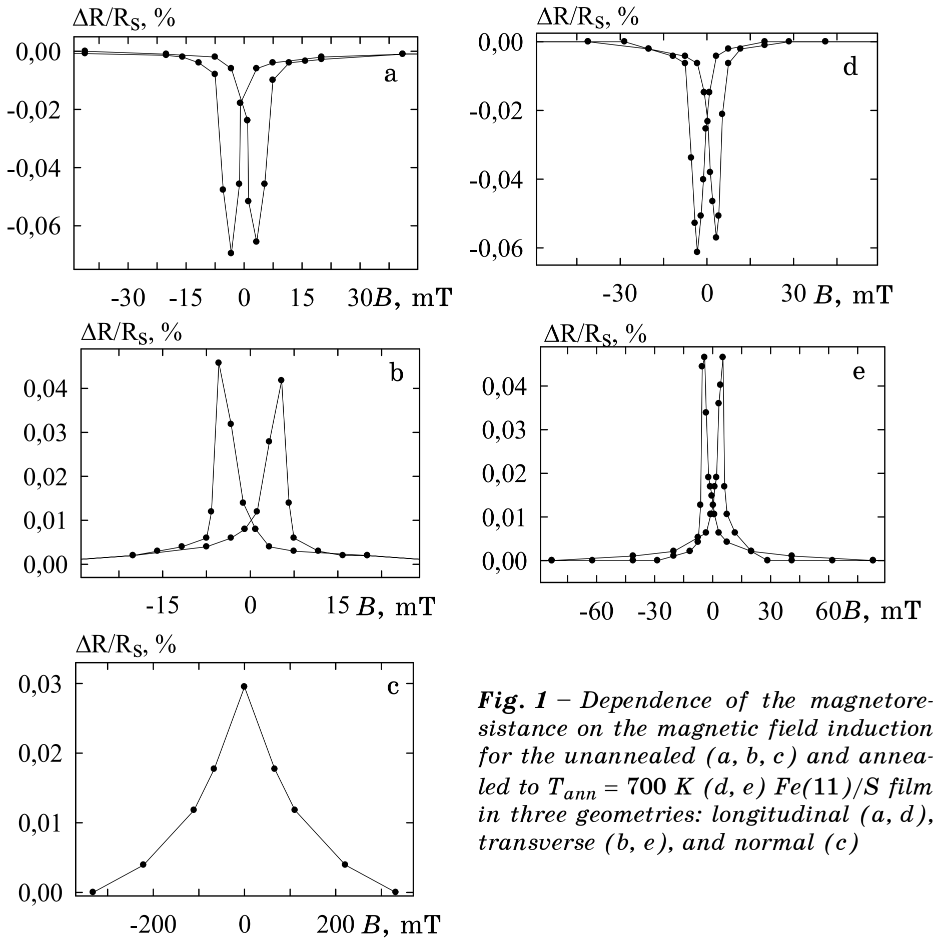

***Fig. 1** – Dependence of the magnetoresistance on the magnetic field induction for the unannealed (a, b, c) and annealed to T_{ann} = 700 K (d, e) Fe(11)/S film in three geometries: longitudinal (a, d), transverse (b, e), and normal (c)*

Film annealing to 700 K does not make considerable changes in the value of B_c and promotes significant decrease (two-fold decrease, on average) in B_s that can be explained by the thermostabilization processes in the grains and domains, and by healing of structural defects. Further annealing to 900 K leads to the essential increase in the values B_c (to 33 mT) and B_s (to 167 mT and more) that is, most probably, conditioned by the substantial coarsening of the grains, and, correspondingly, domains, which require large magnetic fields for the reversal.

Table 1 *– Values of the magnetoresistance for the unannealed and annealed to T_{ann} = 700 and 900 K thin Fe films in different geometries*

Sample	$\Delta R/R_s$, %								
	Longitudinal geometry			Transverse geometry			Normal geometry		
	T = 300 K	T_{ann}, K		T = 300 K	T_{ann}, K		T = 300 K	T_{ann}, K	
		700	900		700	900		700	900
Fe(7)/S	– 0,107	– 0,093	–	0,011	0,026	–	0	0	–
Fe(11)/S	– 0,070	– 0,061	0	0,046	0,047	0	0,030	–	–
Fe(20)/S	– 0,123	– 0,099	– 0,033	0,066	0,084	0,054	0,028	0,035	–
Fe(30)/S	– 0,202	– 0,179	0	0,061	0,092	0,022	0,014	0,014	0
Fe(46)/S	– 0,044	– 0,029	0	0,040	0,052	0,016	0,043	0,030	–
Fe(60)/S	– 0,071	– 0,062	– 0,028	0,065	0,080	0,062	0,047	0,037	0

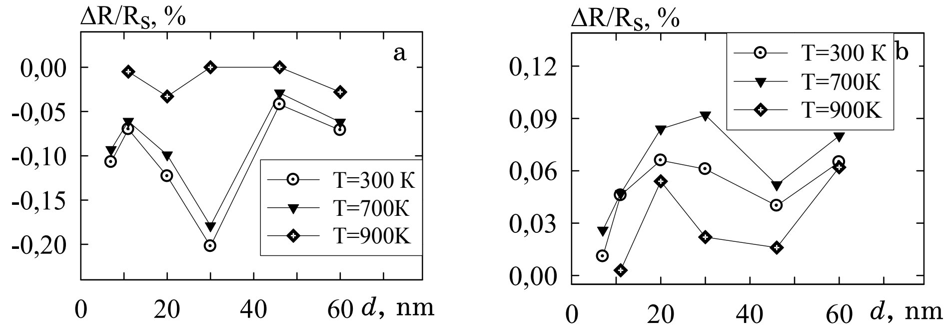

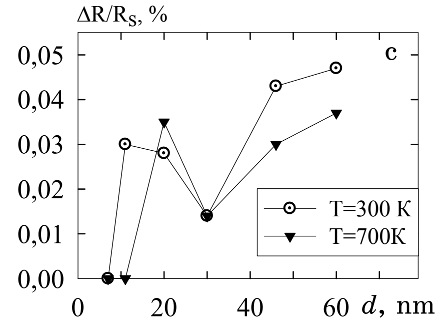

Рис. 2 *– Size dependences of the magnetoresistance for the unannealed and annealed to T_{ann} = 700 and 900 K thin Fe films in three geometries: longitudinal (a), transverse (b), and normal (c)*

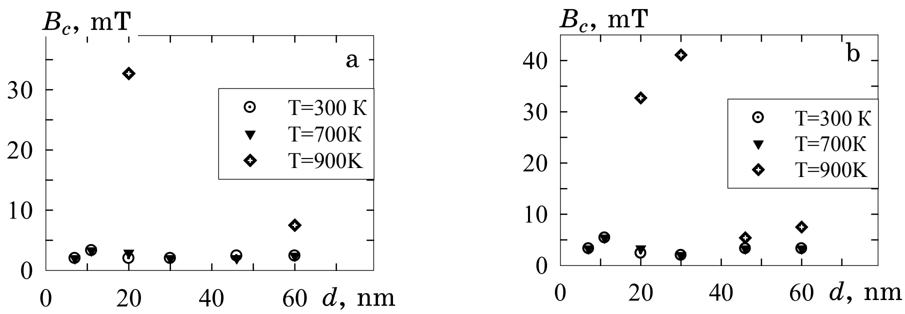

Fig. 3 *– Size dependences of the induction of demagnetizing B_c for the unannealed and annealed to T_{ann} = 700 and 900 K Fe films in the longitudinal (a) and transverse (b) geometries*

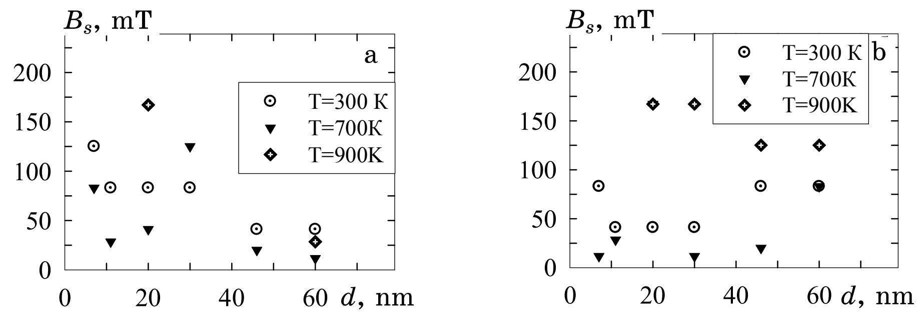

Fig. 4 *– Size dependences of the induction of saturation B_s for the unannealed and annealed to T_{ann} = 700 and 900 K Fe films in the longitudinal (a) and transverse (b) geometries*

Judging from the peaks on the size dependences of the MR, B_c and B_s, it seems that at the thickness $d_{Fe} \cong$ 20-30 nm one can observe the transition from the Neel to the Bloch domain walls, which are characterized by the different width and defect concentration. With the decrease in the film thickness, the domain wall width increases due to the film remagnetization along the lesser demagnetizing factor (into the film plane). Such walls are called the Neel ones [1].

Table 2 – *Values of the induction of demagnetizing B_c and saturation B_s for the unannealed and annealed to T_{ann} = 700 and 900 K Fe films in different geometries*

Sample	Longitudinal geometry						Transverse geometry					
	300 K		700 K		900 K		300 K		700 K		900 K	
	B_c*	B_s*	B_c	B_s	B_c	B_s	B_c	B_s	B_c	B_s	B_c	B_s
Fe(7)/S	2,0	125,1	2,0	83,1	–	–	3,3	83,1	3,3	11,7	–	–
Fe(11)/S	3,3	83,1	3,3	28,5	–	–	5,4	41,1	5,4	28,5	–	–
Fe(20)/S	2,0	83,1	2,9	41,1	32,7; 41,1	167,1	2,4	41,1	3,3	167,1	32,7	>167,1
Fe(30)/S	2,0	83,1	2,0	125,1	–	–	2,0	41,1	2,0	11,7	41,1	>167,1
Fe(46)/S	2,4	41,1	2,0	20,1	–	–	3,3	83,1	3,3	20,1	5,4	125,1
Fe(60)/S	2,4	41,1	2,4	11,7	7,5	28,5	3,3	83,1	3,3	83,1	7,5	>125,1

*B_c and B_s in mT

We should also note that there is the difference in the MR values depending on the measurement geometry. For freshly condensed films, as well as for thermally stabilized ones, dominance of the value of MR is observed for the longitudinal geometry that, probably, can be explained by the shape anisotropy in the studied samples (the film sizes are in the ratio 1:6). In this case, it is more difficult to turn small domains with wide walls in thin films ($d_{Fe} \le$ 30 nm) to saturation in magnetic field that is appeared in the pronounced MR anisotropy and dominance of B_s in the longitudinal geometry. The reversed situation is observed for thicker films (Table 2).

3.2 Multilayers based on Fe and Cr

Multilayer film systems based on Fe and Cr or Cu with the repeated set of Fe/Cr or Fe/Cu fragments (multilayers) were obtained using the technique described in the Section 2. In the most cases a number of fragments was constant and equal to 15. Data of the magnetoresistive measurements in $[Fe/Cr]_n$ multilayers is represented in Table 3 and Table 4. As seen, for two film systems with atomic concentration 45 and 50 at.% of Fe, isotropy of the field dependences $R(B)$ (Fig. 5 and Fig. 6) is typical, i.e., apart from the measurement geometry one can observe the increase in the value of electrical resistance in magnetic field that is the feature of the GMR [3, 4]. For other systems with thin (≤ 2 nm) or relatively thick (4 nm) Cr layers, anisotropy of the field dependences $R(B)$, similarly to Fe films, and dominance of the value of MR in the longitudinal geometry in comparison with two other geometries are typical.

Table 3 *– The MR values in three geometries for the unannealed and annealed to* T_{ann} = 500, 700 *and* 900 *K* $[Fe/Cr]_n$ *multilayers*

Sample	Total thickness, nm	c_{Fe}, at.%	$\Delta R/R_s$, %							
			Longitudinal/transverse geometry				Normal geometry			
			300 K	T_{ann}, K			300 K	T_{ann}, K		
				500	700	900		500	700	900
$[Fe(2,73)/Cr(4,07)]_{15}/S$	102	41	– 0,016/ 0,080	–/–	–/–	– 0,037/ 0,085	0,075	–	–	0,033
$[Fe(2,27)/Cr(2,8)]_{15}/S$	76	45	0,219/ 0,359	0,220/ 0,354	– 0,102/ 0,031	– 0,111/ 0,035	0,207	0,154	0,037	0,054
$[Fe(2,73)/Cr(2,73)]_{15}/S$	82	50	0,375/ 0,413	0,409/ 0,459	– 0,076/ 0,070	– 0,127/ 0,061	0,134	0,103	0,034	0,081
$[Fe(2,8)/Cr(2,2)]_{15}/S$	75	57	– 0,156/ 0,059	– 0,152/ 0,059	– 0,176/ 0,075	–/–	0,047	0,028	0,073	0,033
$[Fe(3,2)/Cr(2)]_{15}/S$	78	62	– 0,026/ 0,142	–/–	–/–	– 0,042 0,096	0,079	–	–	0,056
$[Fe(2,4)/Cr(0,6)]_{15}/S$	45	80	– 0,118/ 0,020	– 0,095 0,009	–/–	–/–	0,021	0	–	–

Table 4 *– Values of the induction of demagnetizing* B_c *and saturation* B_s *in two measurement geometries for the unannealed and annealed to* T_{ann} = 500, 700 *and* 900 *K* $[Fe/Cr]_n$ *multilayers*

Sample	Total thickness, nm	c_{Fe}, at.%	Longitudinal/transverse geometry							
			300 K		annealed to T_{ann}, K					
					500		700		900	
			B_c*	B_s*	B_c	B_s	B_c	B_s	B_c	B_s
$[Fe(2,73)/Cr(4,07)]_{15}/S$	102	41	3,3/ 2,4	41,1/ 167	–/–	–/–	–/–	–/–	7,5/ 3,3	62,1/ >167
$[Fe(2,27)/Cr(2,8)]_{15}/S$	76	45	18,0/ 9,6	>209/ >209	11,7/ 4,1	>167/ >167	3,3/ 4,1	125/ 83,1	3,3/ 7,5	125/ 125
$[Fe(2,73)/Cr(2,73)]_{15}/S$	82	50	3,3/ 6,6	>209/ >209	2,0/ 3,3	>167/ >167	2,0/ 2,0	41,1/ 83,1	2,0/ 5,4	>167/ >125
$[Fe(2,8)/Cr(2,2)]_{15}/S$	75	57	4,1/ 6,6	41,1/ 125,1	3,3/ 7,5	28,5/ 83,1	3,3/ 5,4	28,5/ 20,1	–/–	–/–
$[Fe(3,2)/Cr(2)]_{15}/S$	78	62	3,3/ 3,3	41,1/ 83,1	–/–	–/–	–/–	–/–	20,1/ 3,3	125/ 146
$[Fe(2,4)/Cr(0,6)]_{15}/S$	45	80	2,0/ 7,5	41,1/ 83,1	1,2/ 4,1	41,1/ 11,7	–/–	–/–	–/–	–/–

*B_c and B_s in mT

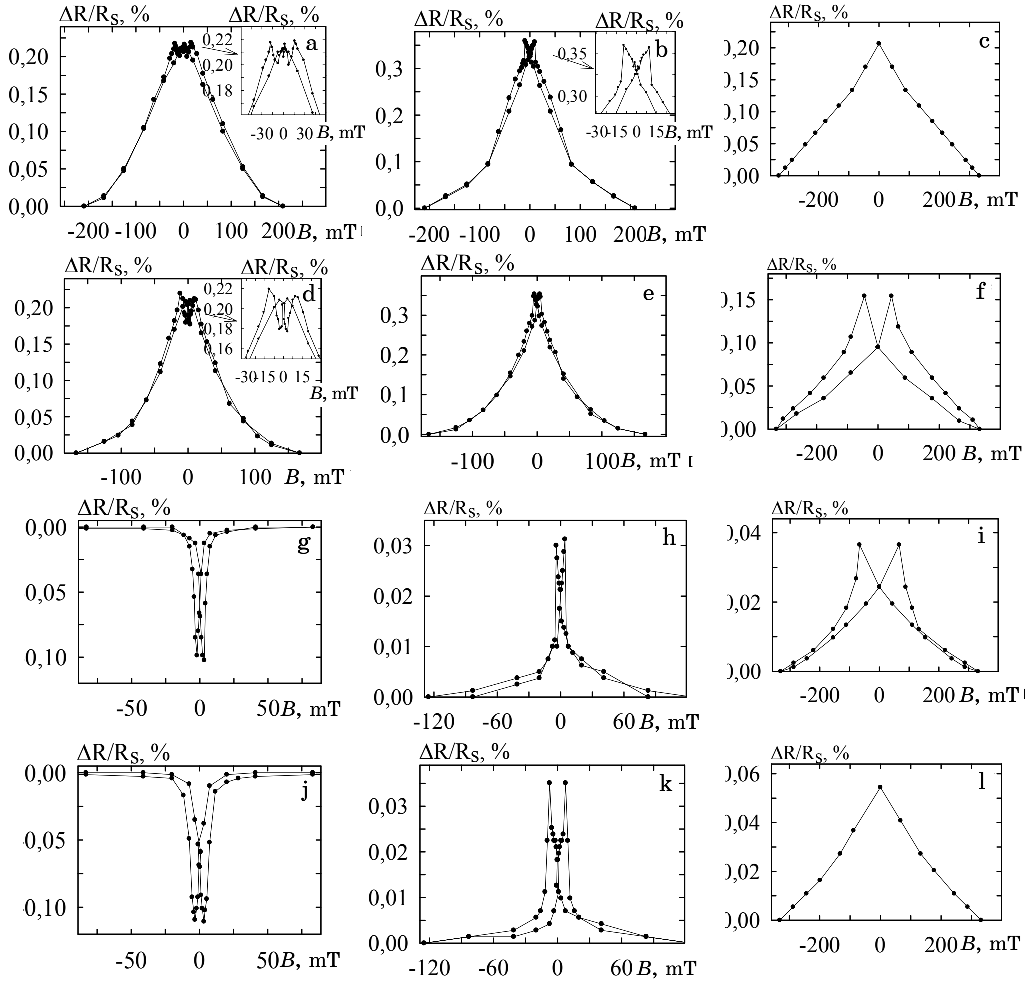

***Fig. 5** – Dependence of the MR on the magnetic field induction for the film system [Fe(2,27)/Cr(2,8)]$_{15}$/S: unannealed (a-c) and annealed to T_{ann} = 500 (d-f), 700 (g-i), and 900 K (j-l) in three geometries: longitudinal (a, d, g, j), transverse (b, e, h, k), and normal (c, f, i, l)*

The authors of [5] have observed the same difference in the value of MR of multilayer [Fe/Cr]$_n$/Fe/S structures for two measurement geometries: the longitudinal and transverse. In the first case the value of MR was 15% more at helium temperatures and 30% more at room temperature. The authors explain such difference by the manifestation of the magnetoresistance anisotropy effect. Anisotropic $\rightarrow$ GMR-structure transition occurs in the case when spin-dependent conduction electron scattering by interfaces magnetic/nonmagnetic material or magnetic granules dominantly contributes to the value of MR in comparison with the scattering by magnetic moments of domains and their walls.

Electron-microscope investigations of $[Fe/Cr]_n$ samples indicate the highly dispersed structure in the case of anisotropic samples and the labyrinthine structure in the case of the samples with the GMR features (Fig. 7), which is typical, for example, for magnetic monocrystalline films with magnetic anisotropy of the type "easy axis" [6] or for nanogranular composites ferromagnetic metal-dielectric [7]. In accordance with the data of [7], the labyrinthine domain structure is the chain of interacting with each other granules, which can be formed into clusters. In thin-film Cr-Fe alloys the same situation, namely, the formation of Fe clusters in Cr matrix at $c_{Fe} > 20$ at.% [8], was observed.

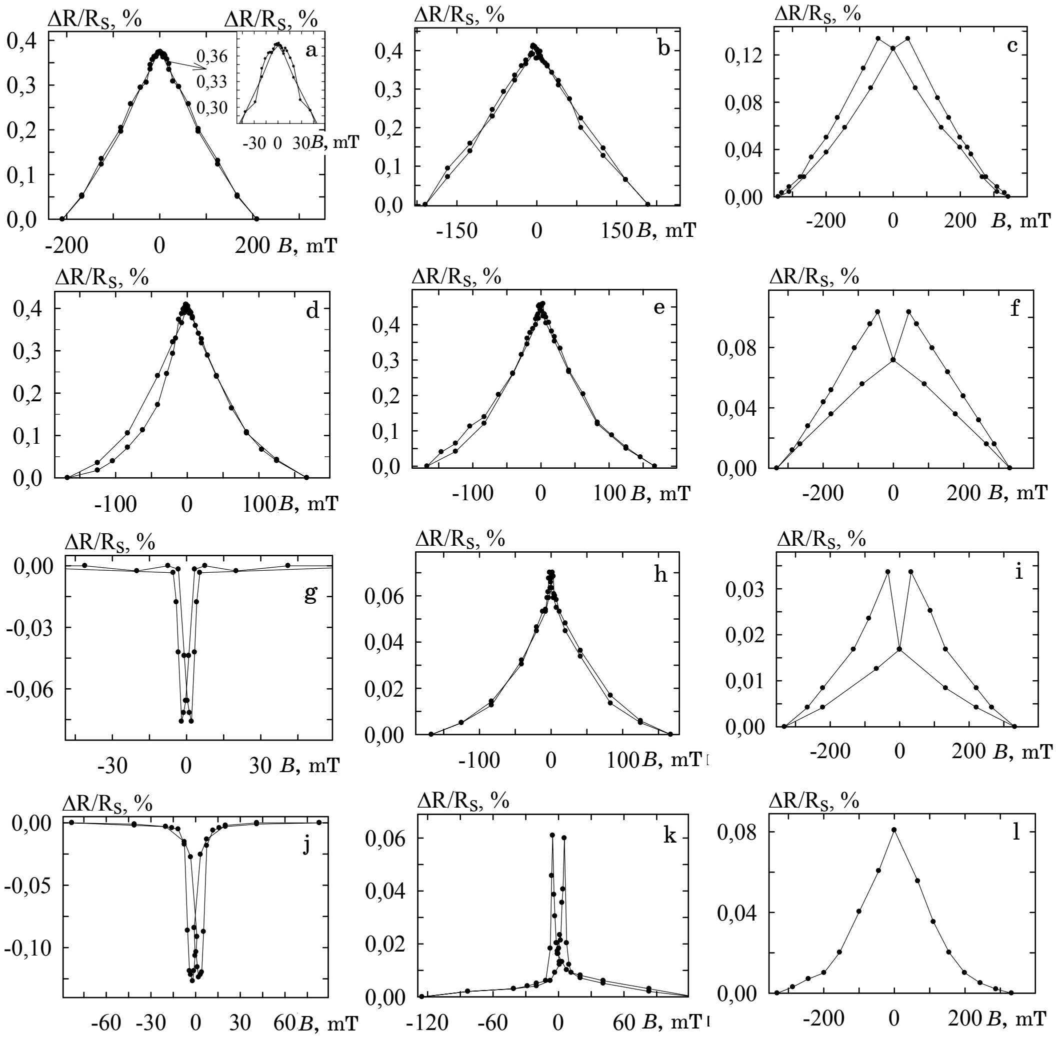

Fig. 6 – Dependence of the MR on the magnetic field induction for the film system $[Fe(2{,}73)/Cr(2{,}73)]_{15}/S$: unannealed (a-c) and annealed to T_{ann} = 500 (d-f), 700 (g-i), and 900 K (j-l) in three geometries: longitudinal (a, d, g, j), transverse (b, e, h, k), and normal (c, f, i, l)

Interpretation of the diffraction patterns from the studied film systems (Table 5) indicates the formation of solid solutions there (α-Fe, Cr) with the lattice parameter close to bulk Fe and Cr both in freshly condensed samples and annealed to different temperatures (0,287-0,289 nm).

Table 5 – *Interpretation of the diffraction patterns from freshly condensed and annealed to* T_{ann} = 500, 700, 900 *K [Fe(*2,73*)/Cr(*2,73*)]*$_{15}$*/S film system*

№	unannealed		T_{ann}, K						hkl	phase
			500		700		900			
	d_{hkl}, nm	a_{hkl}, nm	d_{hkl}, nm	a_{hkl}, nm	d_{hkl}, nm	a_{hkl}, nm	d_{hkl}, nm	a_{hkl}, nm		
1	0,204	0,289	0,205	0,289	0,205	0,289	0,205	0,290	110	s.s.(α-Fe,Cr)
2	0,144	0,288	0,144	0,288	0,145	0,290	0,145	0,290	200	s.s.(α-Fe,Cr)
3	0,118	0,288	0,118	0,288	0,118	0,288	0,118	0,288	211	s.s.(α-Fe,Cr)
4	0,101	0,286	0,102	0,288	0,102	0,288	0,102	0,288	220	s.s.(α-Fe,Cr)
5	0,090	0,286	0,091	0,288	0,091	0,288	0,091	0,288	310	s.s.(α-Fe,Cr)
6	0,082	0,285	0,082	0,285	0,083	0,286	0,083	0,286	222	s.s.(α-Fe,Cr)
$\bar{a}$ (α-Fe,Cr) = 0,287 ± 0,001 nm			$\bar{a}$ (α-Fe,Cr) = 0,288 ± 0,001 nm		$\bar{a}$ (α-Fe,Cr) = 0,288 ± 0,001 nm		$\bar{a}$ (α-Fe,Cr) = 0,289 ± 0,001 nm			
a_0(α-Fe) = 0,287 nm; a_0(Cr) = 0,288 nm [9]										

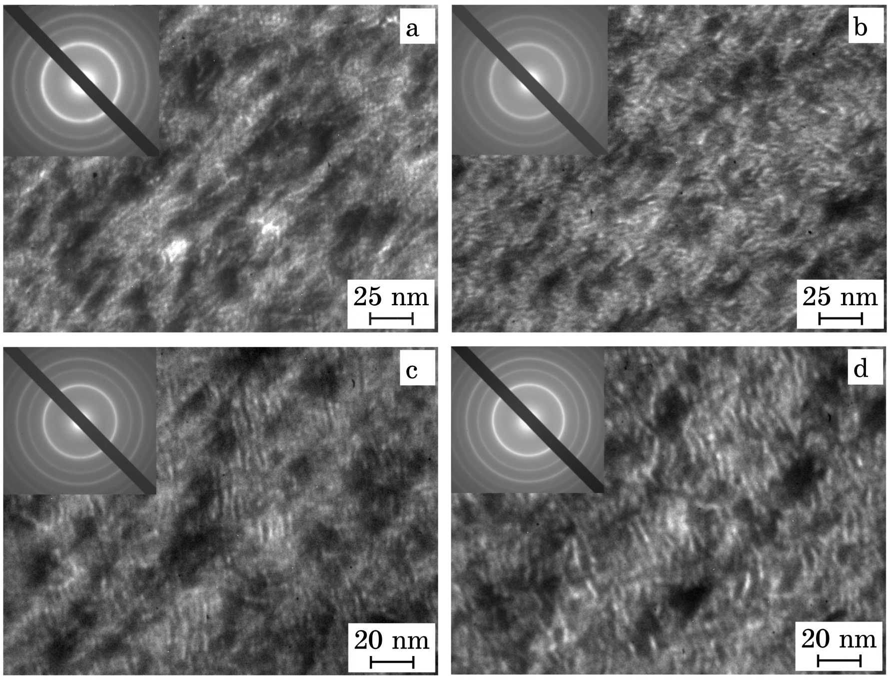

Fig. 7 – *Crystalline structure and diffraction patterns (on the insets) from [Fe(*2,73*)/Cr(*2,73*)]*$_{15}$*/S film system in the unannealed (a) and annealed to* T_{ann} = 500 *(b),* 700 *(c) and* 900 *K (d) and cooled to* 300 *K states*

Thermal treatment of the samples in a wide temperature range 300-900 K in the most cases leads to the slight growth in the value of MR in all three geometries, as well as to the elimination of the GMR features in two samples during annealing over 700 K (Fig. 5g,j; Fig. 6g,j). In this case, coarsening and structuring of labyrinth domains (Fig. 7c,d), whose sizes and interspacings start to exceed the mean free path of conduction electrons [3], are observed on the microscopic images. The authors of [8] also note the influence of the sizes of magnetic clusters: when they exceed the electron mean free path, scattering by clusters does not contribute into the GMR value.

Such behavior of the temperature dependence of MR was observed by the authors of [3] on the example of Co/Cu system and by the authors of [10] on the example of Au-Co alloys when during annealing to 500 K the MR value grows up and then it drops in the high-temperature range.

The question of the thermal treatment influence on the value of the magnetoresistive effect in film systems based on Fe and Cr was considered in the works [8, 11, 12]. Thus, in the case of $[Fe(3,0)/Cr(1,2)]_{10}/S$ multilayers, annealing to the temperatures higher than 570 K leads to the significant growth of an arbitrary magnetization of the sample and sharp decrease of the saturation field that is explained by the dominance of the ferromagnetic (FM) interaction between the magnetic layers in comparison with the antiferromagnetic (AFM) one [11]. The mentioned features correlate with the sharp decrease (almost four-fold decrease) in the MR value at $T_{ann} > 570$ K. Influence of the substrate temperature T_s during the sample production is also important. It is shown in [8] that for the case of Fe-Cr alloys obtained by the method of ion high-frequency sputtering, the optimal temperature T_s is 470 K, at which the MR value is 1,5 times more in comparison with $T_s = 670$ K and is equal to 38% at helium temperatures.

The authors of [12] have shown the influence of the thermal stabilization conditions on the MR value on the example of $[Fe(2,7)/Cr(0,9)]_{25}/S$ multilayer: annealing to 570 K during one hour leaded to the almost two-fold increase in the MR, further annealing during one more hour promoted the MR decrease in comparison with the value before annealing (firstly MR increased from 0,42% to 0,79%, then decreased to 0,33%). Based on the cross-section microscopy data, the obtained results for MR are explained by the smoothing of interfaces in the first case (that has amplified AFM interaction between Fe layers) and intensive diffusion processes in the second case (that has promoted the increase in the roughness of Fe/Cr interfaces and leaded to the dominance of FM interaction). The coercitivity and saturation field data in $[Fe/Cr]_n$ multilayers is represented in Table 4. It is necessary to note the large values of B_s in systems with the GMR features (> 200 mT) that is typical for multilayers with spin-dependent electron scattering [13]. Hysteresis features in these films are expressed in the presence of double peaks on the magnetoresistive loops (Fig. 6a,b,d) and sufficiently large values of B_c (3,3-18,0 mT) that can be explained by the remagnetization of Fe layers by non-coherent rotation of their magnetization [3]. The considerable decrease in the B_s value (to 30-40 mT) is observed in anisotropic samples based on Fe/Cr that essentially influences the values of MR sensitivity to magnetic field. In this case, the typical for all samples growth in B_s is observed only during annealing to 900 K that is, probably, connected with the structure and phase state of the system, namely, with the partial decomposition of α-Fe,Cr solid solution [16].

3.3 Multilayers based on Fe and Cu

Anisotropy of the field dependences $R(B)$ and, correspondingly, $\Delta R/R_s(B)$ (see Table 6) is observed in multilayer film systems based on Fe and Cu, and it can be explained by the different behavior of the magnetization vectors along the easy or hard magnetization axes [17]. The stated fact is typical for the samples with atomic concentration of Fe atoms $c_{Fe} > 50\%$. We should note that for the mentioned samples the MR value does not exceed 0,05% in the most cases. At smaller values of c_{Fe} the anisotropy vanishes (Fig. 8), and the MR value substantially increases ($\Delta R/R_s = 0,1\text{-}0,2\%$ for $[Fe(1,6)/Cu(1,73)]_{30}/S$ ($c_{Fe} = 48\%$)) that can indicate the GMR presence in Fe/Cu-based multilayers. As seen from Table 6, at the thickness of Cu sublayer of the order of 0,5-1 nm, which corresponds to the minimum on the oscillation dependence for MR [18], a significant drop of the MR value is observed.

Table 6 – *The MR values in three geometries for the unannealed and annealed to T_{ann} = 850 K $[Fe/Cu]_n$ multilayers*

Sample	Total thickness, nm	c_{Fe}, at.%	Magnetoresistance			
			Longitudinal geometry		Transverse geometry	
			unanneal.	anneal. to 850 K	unanneal.	anneal. to 850 K
$[Fe(1,6)/Cu(1,73)]_{30}/S$	100	48	0,107	0,043	0,184	0,074
$[Fe(1,4)/Cu(1,67)]_{15}/S$	46	46	– 0,140	– 0,063	0,055	0,032
$[Fe(2,2)/Cu(1,67)]_{15}/S$	58	57	– 0,139	0	0,037	0,030
$[Fe(2,87)/Cu(1,73)]_{15}/S$	69	62	– 0,124	– 0,116	0,010	0,014
$[Fe(1,93)/Cu(1,73)]_{15}/S$	55	53	– 0,116	– 0,103	0,020	0,022
$[Fe(1,93)/Cu(1,03)]_{30}/S$	89	65	– 0,025	–	0,014	–
$[Fe(2)/Cu(0,6)]_{15}/S$	39	77	– 0,048	– 0,015	0,015	0,033
$[Fe(2,13)/Cu(0,6)]_{15}/S$	41	78	– 0,051	– 0,006	0,086	– 0,005
$[Fe(2,53)/Cu(0,6)]_{15}/S$	47	81	– 0,063	– 0,026	0,118	0,044
$[Fe(2,26)/Cu(0,52)]_{23}/S$	64	81	– 0,051	– 0,047	0,025	0,040
$[Fe(3,67)/Cu(0,4)]_{15}/S$	61	90	– 0,023	0,010	0,043	0,023

We also have to note the presence of the hysteresis and magnetic saturation in small fields (Table 7) on the magnetoresistive dependences. Thermal treatment of the samples leads to the increase in the magnetoresistive effect in the transverse geometry and to the decrease in the effect in the longitudinal geometry. In this case in the samples with $d_{Cu} < 1$ nm the considerable increase in the induction of demagnetizing (from 1-2 mT to 20-40 mT in the longitudinal and from 7,5 mT to 40 mT in the transverse geometry) and the increase in the saturation field are observed.

Investigation of the structure and phase state of Fe/Cu-based film systems denotes the formation of a solid solution there in contrast to the two-layer systems, which we have studied before, with the relatively thick layers (~ 20-50 nm), where the individuality of separate layers remains to a considerable degree [19]. In this case, at the layer thicknesses $d_{Fe} \leq 1,5$ nm the (α-Fe,Cu) solid solution is formed based on the fcc-lattice (Fig. 9), and in the thickness range $1,5 < d_{Fe} \leq 2$ nm – based on the bcc-lattice (Fig. 10 and Table 8). In the first case we did not observe the magnetoresistive effect and this is probably connected with very small effective thicknesses of Fe layers and Cu sublayers (< 1 nm).

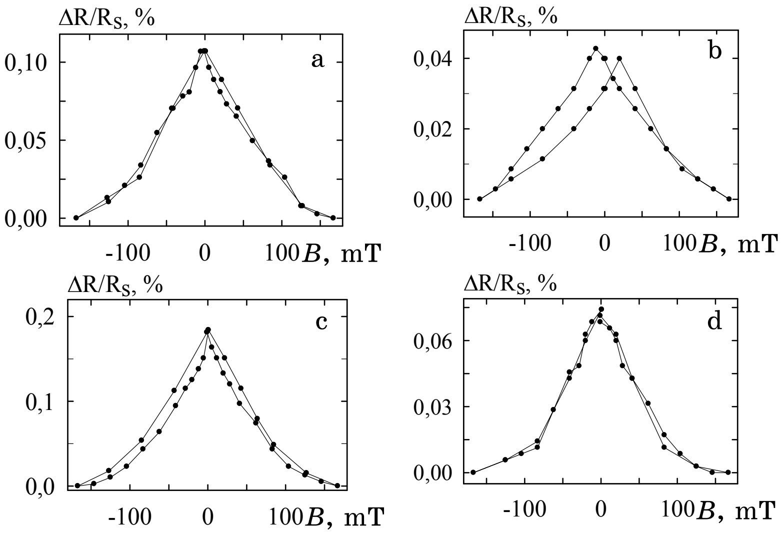

Fig. 8 *– Dependence of the MR on the magnetic field induction for the film system [Fe(*1,6*)/Cu(*1,73*)]*$_{30}$*/S: unannealed (a, c) and annealed to* T_{ann} = 850 *K (b, c) in the longitudinal (a, b) and transverse (c, d) geometries*

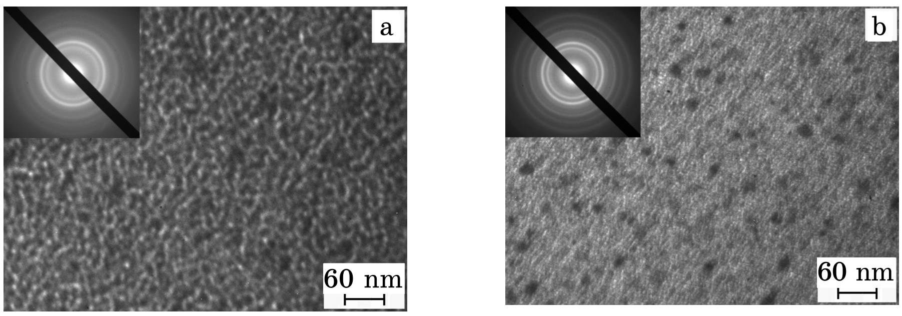

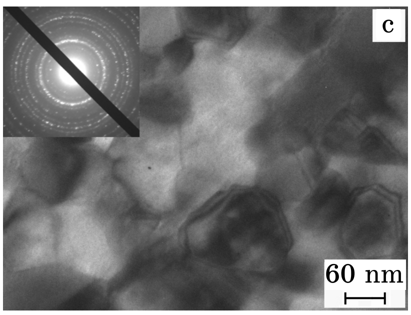

Fig. 9 *– Crystalline structure and diffraction patterns (on the insets) from the film system [Fe(*0,6*)/Cu(*0,3*)]*$_{70}$*/S in the unannealed (a) and annealed to* T_{ann} = 500 *(b) and* 900 *K (c) and cooled to* 300 *K states*

***Table 8** – Interpretation of the diffraction patterns from freshly condensed and annealed to T_{ann} = 500, 850 K [Fe(1,6)/Cu(1,73)]$_{30}$/S film system*

№	unannealed		T_{ann}, K				hkl	phase
			500		850			
	d_{hkl}, nm	a_{hkl}, nm	d_{hkl}, nm	a_{hkl}, nm	d_{hkl}, nm	a_{hkl}, nm		
1	0,204	0,288	0,205	0,290	0,206	0,291	110	s.s.(Cu,α-Fe)
2	0,145	0,290	0,146	0,292	0,147	0,294	200	s.s.(Cu,α-Fe)
3	0,117	0,286	0,117	0,287	0,118	0,289	211	s.s.(Cu,α-Fe)
4	0,102	0,288	0,103	0,291	0,103	0,291	220	s.s.(Cu,α-Fe)
5	0,091	0,288	0,091	0,287	0,091	0,288	310	s.s.(Cu,α-Fe)
$\bar{a}$ (Cu,α-Fe) = 0,288 ± 0,001 nm			$\bar{a}$ (Cu,α-Fe) = 0,289 ± 0,001 nm			$\bar{a}$ (Cu,α-Fe) = 0,290 ± 0,001 nm		
a_0(α-Fe) = 0,287 nm; a_0(Cu) = 0,361 nm [9]								

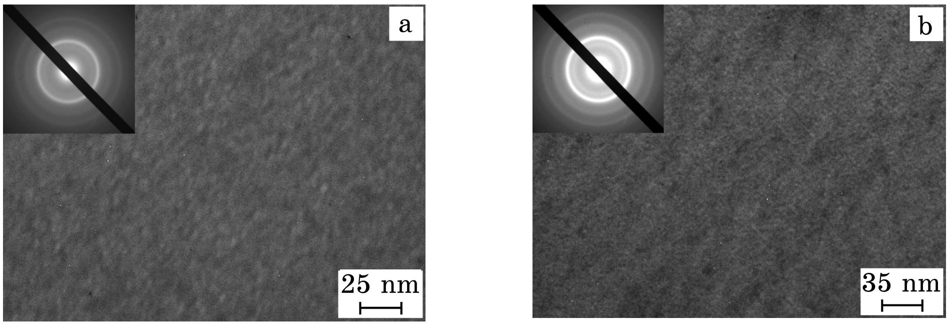

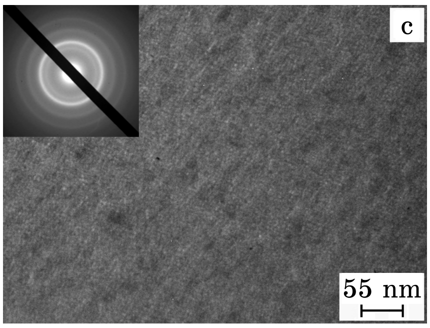

***Fig. 10** – Crystalline structure and diffraction patterns (on the insets) from the film system [Fe(1,6)/Cu(1,73)]$_{30}$/S in the unannealed (a) and annealed to T_{ann} = 500 (b) and 850 K (c) and cooled to 300 K states*

4. DISCUSSION OF THE RESULTS

Besides the MR value, the value of the saturation field is of a great importance while choosing the film system as the element base of microelectronics. The minimum values of B_s are reached in spin-valve structures due to the difference in the coercitivity values of magnetic layers with different thickness or made of different materials [13]. In the studied multilayers the value of the saturation field can be some times reduced by the thermal treatment of the sample (in this case, the larger T_{ann} is, the sharper decrease in the value of B_s is). But it is also necessary to take into account the drop in the MR value with the increase in the annealing temperature, which can be both the insignificant (almost 1,5-fold decrease in the case of Fe_xAg_{100-x} alloys [13] and Co/Cu/Co three-ply [2]) and ten-fold (for example, in the case of $[Co/Ni/Cu]_n$ system [14]). Therefore, in some works devoted to the application of the GMR-structures in sensor technology and production of read/record heads [13, 15], the notion of the film system to magnetic field sensitivity is introduced, and its maximum value will be defined by the formula

$$S_B = \left|\frac{(\Delta R\ /\ R(B_S))_{\max}}{\Delta B}\right|,$$

where $(\Delta R/R(B_S))_{\max}$ is the maximum value of the MR; ΔB is the change of the magnetic field induction on the saturation B_s (or on the maximum value) to the demagnetizing B_c, which, in fact, is equal to $\Delta B = B_s + B_c$.

The value of S_B is measured in %/T (or in %/(kA/m) [13]) and gives an idea of the relationship of the MR values and saturation field.

In Fe films the value of the magnetoresistive effect to magnetic field sensitivity grows during annealing to 500 K and sharply decreases with further annealing to 900 K (Table 9). Exceptions are the Fe films with the thicknesses 20 nm and 30 nm, at which, most probably, the change in the type of domain walls occurs.

Table 9 *– The values of the sensitivity S_B in different measurement geometries for the unannealed and annealed to T_{ann} = 700 and 900 K thin Fe films*

Sample	S_B, %/T					
	Longitudinal geometry			Transverse geometry		
	T = 300 K	T_{ann}, K		T = 300 K	T_{ann}, K	
		700	900		700	900
Fe(7)/S	0,84	1,09	–	0,13	1,73	–
Fe(11)/S	0,81	1,92	–	0,99	1,39	–
Fe(20)/S	1,44	2,25	0,16	1,52	0,49	0,27
Fe(30)/S	2,37	1,41	–	1,41	6,71	0,10
Fe(46)/S	1,01	1,31	–	0,46	2,22	0,12
Fe(60)/S	1,63	4,39	0,78	0,75	0,92	0,47

In $[Fe/Cr]_n$ samples, where the GMR features are observed, sensitivity S_B varies in the limits (0,2-2,7)%/T. In this case sensitivity increases on average by 20% during annealing to 500 K and sharply decreases with further annealing to 700 or 900 K (Table 10). In other samples with the anisotropy of the field dependences $R(B)$ the same temperature dependence of S_B, which is typical for Fe films, is observed.

Another situation takes place in Fe/Cu film system. In the samples with $d_{Cu} \approx 1,7$ nm the value of S_B reaches significant values (3-14)%/T and is not almost changed after annealing to 850 K (see Table 11). In this case, the decrease in S_B is marked during annealing in the systems with $d_{Cu} < 1$ nm that indicates the temperature instability of the magnetoresistive effect.

Table 10 *– The values of the sensitivity S_B in different measurement geometries for the unannealed and annealed to T_{ann} = 500, 700, and 900 K thin Fe/Cr films*

Sample	Total thickness, nm	c_{Fe}, at.%	S_B, %/T							
			Longitudinal geometry				Transverse geometry			
			unanneal.	T_{ann}, K			unanneal.	T_{ann}, K		
				500	700	900		500	700	900
$[Fe(2,73)/Cr(4,07)]_{15}/S$	102	41	0,36	–	–	0,53	0,47	–	–	< 0,50
$[Fe(2,27)/Cr(2,8)]_{15}/S$	76	45	< 0,96	< 1,23	0,79	0,86	< 1,64	< 2,07	0,35	0,26
$[Fe(2,73)/Cr(2,73)]_{15}/S$	82	50	< 1,77	< 2,42	1,76	< 0,75	< 1,91	< 2,69	0,82	< 0,47
$[Fe(2,8)/Cr(2,2)]_{15}/S$	75	57	3,45	4,78	5,53	–	0,45	0,65	2,94	–
$[Fe(3,2)/Cr(2)]_{15}/S$	78	62	0,58	–	–	0,29	1,64	–	–	0,64
$[Fe(2,4)/Cr(0,6)]_{15}/S$	45	80	2,74	2,24	–	–	0,22	0,57	–	–

Table 11 *– The values of the sensitivity S_B in different measurement geometries for the unannealed and annealed to T_{ann} = 850 K thin Fe/Cu films*

Sample	Total thickness, nm	c_{Fe}, at.%	S_B, %/T			
			Longitudinal geometry		Transverse geometry	
			unannealed	T_{ann} = 850 K	unannealed	T_{ann} = 850 K
$[Fe(1,6)/Cu(1,73)]_{30}/S$	100	48	0,64	0,24	1,10	0,44
$[Fe(1,4)/Cu(1,67)]_{15}/S$	46	46	3,31	2,19	6,32	0,38
$[Fe(2,2)/Cu(1,67)]_{15}/S$	58	57	1,08	–	0,43	0,18
$[Fe(2,87)/Cu(1,73)]_{15}/S$	69	62	3,00	5,69	0,35	0,11
$[Fe(1,93)/Cu(1,73)]_{15}/S$	55	53	14,87	13,21	0,12	0,26
$[Fe(1,93)/Cu(1,03)]_{30}/S$	89	65	0,28	–	0,16	–
$[Fe(2)/Cu(0,6)]_{15}/S$	39	77	1,08	0,10	0,42	0,16
$[Fe(2,13)/Cu(0,6)]_{15}/S$	41	78	0,30	0,03	0,51	0,02
$[Fe(2,53)/Cu(0,6)]_{15}/S$	47	81	1,42	0,20	5,34	0,25
$[Fe(2,26)/Cu(0,52)]_{23}/S$	64	81	1,21	0,57	0,58	0,24
$[Fe(3,67)/Cu(0,4)]_{15}/S$	61	90	0,26	0,12	0,50	0,12

5. CONCLUSIONS

Based on the analysis of the experimental results we can conclude the following:

1. The anisotropy of the field dependences $R(B)$ is typical for ferromagnetic Fe films. In this case, for the freshly condensed films, as well as for the thermally stabilized ones, dominance in the value of MR is observed for the longitudinal geometry that, probably, can be explained by the anisotropy of the sample geometry. Thermal annealing of the samples leaded to the insignificant increase (T_{ann} = 700 K) and drop of the amplitude $\Delta R/R_s$ (900 K) in the transverse geometry and to the smooth de-crease in $\Delta R/R_s$ in the whole temperature range in the longitudinal and normal geometries.
2. Isotropy of the filed dependences $R(B)$ is typical for film Fe/Cr systems with concentration 45 and 50 at.% of Fe that is the GMR feature. Thermal treatment of the samples in a wide temperature range (300-900 K) in the most cases leaded to the insignificant growth in the MR value in all three geometries and to the removal of the GMR features in two samples under annealing above 700 K.

3. Electron-microscopic investigations of $[Fe/Cr]_n$ samples indicate the fine-dispersed structure in the case of anisotropic samples and the labyrinthine structure in the case of the samples with the GMR features. Interpretation of the diffraction patterns from the studied film systems implies the formation of solid solutions (α-Fe, Cr) there.
4. Small value (0,05%) of the magnetoresistive effect and its anisotropy at the concentration more than 50 at.% of Fe, which vanishes with the decrease in c_{Fe}, is typical for film Fe/Cu system. In this case, the value of MR substantially increases (up to 0,2%) that can indicate the presence of the GMR in this system. Thermal treatment of the samples, increase in the thickness of non-magnetic sublayer, and decrease in the thickness of magnetic layer lead to the total decrease in the MR value.
5. Study of the structure and phase state of nanoscale multilayer systems based on Fe and Cu shown the presence of a solid solution (α-Fe,Cu) based on the fcc-Fe lattice for the layer thicknesses $d_{Fe} \leq 1,5$ nm and the bcc-(α-Fe) lattice in the thickness range $1,5 < d_{Fe} \leq 2$ nm.

The research has been performed under the financial support of the Ministry of Education and Science of Ukraine (Grant No 0109U001387, 2009-2011).

REFERENCES

1. V. Andre, L. Valenta, Z. Malek, *Tonkie ferromagnitnye plenki* (M.: Mir: 1964).
2. L.A. Chebotkevich, Yu.D. Vorob'ev, I.N. Burkova, A.V. Kornilov, *Phys. Met. Metallogr.* **89** No3, 263 (2000).
3. V.O. Vas'kovskii, A.A. Yuvchenko, V.N. Lepalovskii, N.N. Shchegoleva, A.V. Svalov, *Phys. Met. Metallogr.* **93** No3, 232 (2002).
4. I. Bakonyi, L. Peter, *Prog. Mater. Sci.* **55,** 107 (2010).
5. J. Barnas, A. Fuss, R.E. Camlej, P. Grunberg, W. Zinn, *Phys. Rev. B* **42,** 8110 (1990).
6. A.P. Ges', V.V. Fedotova, A.K. Bogush, T.A. Gorbachevskaya, *JETP Lett.* **52,** 476 (1990).
7. O.V. Stognei, A.V. Sitnikov, Yu.E. Kalinin, S.F. Avdeev, M.N. Kopytin, *Phys. Solid State* **49,** 164 (2007).
8. T. Sugawara, K. Takanashi, K. Hono, H. Fujimori, *J. Magn. Magn. Mater.* **159,** 95 (1996).
9. S.S. Gorelik, L.N. Rastorguev, Yu. A. Skakov, *Rentgenograficheskii i elektronograficheskii analiz metallov* (M.: GNTI: 1963).
10. M. Kitada, *J. Magn. Magn. Mater.* **208,** 244 (2000).
11. V. Korenivski, K.V. Rao, D.M. Kelly, I.K. Schuller, K.K. Larsen, J. Bottiger, *J. Magn. Magn. Mater.* **140-144,** 549 (1995).
12. E.M. Ho, A.K. Petford-Long, *J. Magn. Magn. Mater.* **156,** 65 (1996).
13. S. Tumanski, *Thin film magnetoresistive sensors* (London: IOP Publishing: 2001).
14. V.B. Loboda, V.O. Kravchenko, Yu. O. Shkurdoda, *J. Nano- Electron. Phys.* **1** No2, 18 (2009).
15. K.-M.H. Lenssen, H.W. van Kesteren, Th. G.S.M. Rijks, J.C.S. Kools, M.C. de Nooijer, R. Coehoorn, W. Folkerts, *Sens. Actuat. A-Phys.* **60,** 90 (1997).
16. O.V. Synashenko, A.I. Saltykova, I.Yu. Protsenko, *J. Nano- Electron. Phys.* **1** No2, 79 (2009).
17. V.A. Buravihin, V.S. Khristosenko, *Fizika magnitnyh plenok* (Irkutsk: Tipografiya IOUP: 1967).
18. F. Petroff, A. Barthelemy, D.H. Mosca, D.K. Lottis, A. Fert, P.A. Schroeder, W.P. Pratt, R. Loloee, S. Lequien, *Phys. Rev. B* **44,** 5355 (1991).
19. S.I. Protsenko, I.V. Cheshko, D.V. Velikodny, I.M. Pazuha, L.V. Odnodvorets, I.Yu. Protsenko, O.V. Synashenko, *Uspehi fiz. met.* **8** No4, 247 (2007).